inter·noise 94
YOKOHAMA-JAPAN, AUGUST 29-31

AN EVALUATION OF ACTIVE NOISE ATTENUATION IN RECTANGULAR ENCLOSURES

Scott D. Sommerfeldt and John W. Parkins

Applied Research Laboratory and Graduate Program in Acoustics, The Pennsylvania State University, P.O. Box 30, State College, PA, USA 16804

I-INCE Subject Classification Number: 38.2

INTRODUCTION

A number of current problems of interest in active noise control involve the need to control the sound field in an enclosure. Attenuating the sound pressure at a microphone in the enclosure typically results in a relatively small region of control, often referred to as a zone of silence. In an effort to increase the region of control for practical applications, as many as 32-48 microphones have been used to achieve a broader region of control [1,2,3]. In an attempt to simplify the control architecture, an alternative control method for achieving a more global control of the field has been developed. The method is based on sensing and minimizing the total energy density at discrete locations, rather than the squared pressure as has been done previously.

Previous work using this energy density method in one-dimensional enclosures has indicated that significant improvement in the overall attenuation may be possible [4,5]. This improvement can be attributed to the fact that sensing the energy density provides the capability of observing all modes contributing to the acoustic field. As a result of the increased observability, the spillover problem that often leads to localized control when minimizing the pressure field is largely avoided.

In this paper, the energy density control approach is extended to three-dimensional rectangular enclosures. Numerical results are presented to compare the attenuation of the global potential energy that can be achieved by minimizing the energy density and the acoustic pressure in the enclosure. These results are also compared with the control that one would achieve by minimizing the total potential energy in the enclosure, which has been suggested as the optimal theoretical solution [6].

THEORETICAL DEVELOPMENT

For an active control application, the acoustic field in a rectangular enclosure can be thought of as consisting of two components: the pressure due to the primary source(s), and the pressure due to the secondary source(s). In general, the control that can be achieved in the enclosure will depend on the location of the sources, the location of the error sensors used, and the choice of the performance function chosen for the control system. The purpose of this paper is to compare the control that can be achieved using several different performance functions, for a given arbitrary source and sensor

configuration. As a result, for the results shown below, there has been no attempt to optimize any of the source or sensor locations. The focus is simply to compare the performance that can be realized for a given configuration. This corresponds to the situation that often occurs in practice, where one has limited control over the possible locations for sources and sensors. Given this objective, a single primary source and a single control source are also assumed to simplify the configuration.

The pressure field in the rectangular enclosure can be represented in terms of the modes of the enclosure as

$$p(\vec{x}) = \sum_{N=0}^{\infty} (A_N + B_N Q_c) \Psi_N(\vec{x}) .$$

(1)

Here, N denotes a triple sum over the indices (l, m, n) corresponding to the x-, y-, and z-directions. The functions Ψ_N correspond to the eigenfunctions of the enclosure, Q_c designates the complex control source strength, and the coefficients A_N and B_N are the modal coefficients associated with the primary field and the secondary control field, respectively. (The source strength of the primary source is included in the A_N coefficients.) The objective of the active control system is to optimize the value of the source strength, Q_c, so as to minimize a chosen performance function.

In this paper, three different performance functions for the control system are investigated to compare their global performance. The first performance function corresponds to the global potential energy in the enclosure. This function was suggested by Nelson, et al. [6], since it provides a global measure of the energy in the field. While this approach is attractive for analytical work, it is problematic for experimental implementation, due to the lack of appropriate sensors to obtain a global measure of the potential energy. The second performance function investigated corresponds to the squared pressure at a discrete location(s). This is the approach most often taken in practice, and corresponds to minimizing the pressure magnitude at discrete points in the enclosure. While this approach lends itself well to experimental implementation, it often leads to the production of localized zones of silence, rather than the broad global attenuation often desired. The third performance function investigated corresponds to minimizing the total energy density at a discrete location(s). This approach also makes use of a local measurement, but the measurement of energy density potentially yields more global information than is obtained from a pressure measurement. These three performance functions can be expressed as:

$$J_{pe} = \int \frac{p^2}{2\rho c^2} dV$$

$$J_p = \sum_{i=1}^{I} p^2(\vec{x}_i)$$

(2)

$$J_{ed} = \sum_{i=1}^{I} \frac{p^2(\vec{x}_i)}{2\rho c^2} + \frac{\rho}{2} \vec{v}(\vec{x}_i) \cdot \vec{v}(\vec{x}_i) .$$

Here, the subscript *pe* refers to potential energy, the subscript *p* refers to the squared pressure, and the subscript *ed* refers to the energy density, and I indicates the number of error sensors used.

Using the expression for the pressure given in Eq. (1), these three performance functions can be minimized to yield the optimal control source strengths. The results of

this minimization can be expressed as:

$$Q_{c,pe} = - \frac{\sum\limits_{N=0}^{\infty} B_N^* A_N}{\sum\limits_{N=0}^{\infty} B_N^* B_N}$$

$$Q_{c,p} = - \frac{\sum\limits_{i=1}^{I} \sum\limits_{N=0}^{\infty} A_N \Psi_N(\vec{x}_i)}{\sum\limits_{i=1}^{I} \sum\limits_{N=0}^{\infty} B_N \Psi_N(\vec{x}_i)} \qquad (3)$$

$$Q_{c,ed} = - \frac{\sum\limits_{i=1}^{I} \sum\limits_{N=0}^{\infty} \sum\limits_{M=0}^{\infty} A_N B_M^* \left[\Psi_N(\vec{x}_i) \Psi_M(\vec{x}_i) + \frac{1}{k^2} \nabla\Psi_N(\vec{x}_i) \cdot \nabla\Psi_M(\vec{x}_i) \right]}{\sum\limits_{i=1}^{I} \sum\limits_{N=0}^{\infty} \sum\limits_{M=0}^{\infty} B_N B_M^* \left[\Psi_N(\vec{x}_i) \Psi_M(\vec{x}_i) + \frac{1}{k^2} \nabla\Psi_N(\vec{x}_i) \cdot \nabla\Psi_M(\vec{x}_i) \right]}$$

In the results that follow, the optimal control source strengths have been determined for each of the three performance functions investigated, and with these source strengths, the acoustic pressure throughout the enclosure can be determined by means of Eq. (1).

NUMERICAL MODEL

To investigate the control of the acoustic field in an enclosure, the global potential energy in a rigid rectangular enclosure was determined numerically, both without and with control, for each of the three performance functions shown in Eq. (2). The assumption of rigid boundaries yields eigenfunctions of the form

$$\Psi_N(\vec{x}_i) = \cos\left(\frac{l \pi x_i}{L_x} \right) \cos\left(\frac{m \pi y_i}{L_y} \right) \cos\left(\frac{n \pi z_i}{L_z} \right) \qquad (4)$$

where L_x, L_y, L_z are the dimensions of the enclosure along the three axes. The dimensions of the enclosure modeled are 1.93 m × 1.54 m × 1.22 m, which corresponds to an existing experimental enclosure at Penn State University. Given the dimensions of the enclosure and the source and error sensor locations, which were arbitrarily chosen, the modal coefficients A_N and B_N were first determined, from which the optimal source strengths as given in Eq. (3) can be determined. From the optimal source strengths, the global potential energy in the enclosure can be calculated. Due to the orthogonality of the modes, the potential energy can be expressed as

$$E_p = \frac{V}{4\rho c^2} \sum\limits_{N=0}^{\infty} \left(A_N + B_N Q_c \right)\left(A_N^* + B_N^* Q_c^* \right) . \qquad (5)$$

As well, the pressure field in the enclosure was also determined using the calculated optimal source strengths to gain insight into the global control effects associated with each of the performance functions investigated. In computing the pressure field and global potential energy, the infinite sums indicated in Eqs. 1, 3, and 5 were truncated to include
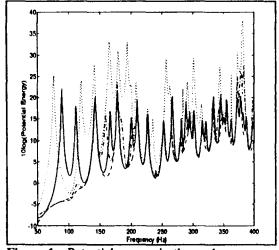
the first 1120 modes.

RESULTS

For the results presented here, a single primary source and a single control source have been used. The primary source was arbitrarily located at $(x,y,z) = (0.1, 0.4, 0.4)$, and the control source was located at $(x,y,z) = (1.4, 1.0, 1.0)$. As mentioned previously, no attempt was made to optimize these locations. Given that there is only a single control source, it is not possible for the control source to significantly attenuate the global energy at frequencies where multiple modes contribute significantly to the acoustic field. However, it is still reasonable to look at the control effects using the three performance functions chosen to gain insight into the global nature of the control schemes. This is particularly true since one of the performance functions is the global potential energy, which will yield the minimum overall potential energy in the enclosure for any chosen configuration.

For minimizing the potential energy, no error sensor is used, as the performance measure is the global energy. For minimizing the squared pressure and the energy density, a single error sensor was used, located at $(x,y,z) = (1.2, 0.6, 0.6)$.

A global measure of the control is given by the potential energy in the enclosure both before and after the control is applied. Figure 1 shows the potential energy in the enclosure, as calculated from Eq. (5), as a function of frequency. From these results, it can be seen that minimizing the potential energy yields the lowest global energy, as is to be expected. However, minimizing the energy density at the single point chosen yields potential energy results that are comparable to minimizing the potential energy at most of the frequencies shown here. On the other hand, minimizing the squared pressure leads to an increase in the global potential energy in the enclosure at most frequencies. This can be seen more clearly in Figure 2, which shows the attenuation in the potential energy that is achieved using each of the three control approaches. The negative values of attenuation at most frequencies for the squared pressure control indicate an increase in the energy in the enclosure, while controlling the energy density provides attenuation of the global field that approximates the control of potential energy reasonably well.

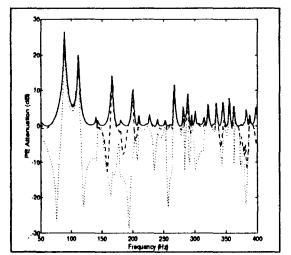Additional insight into the control effect achieved with each of the control

Figure 1. Potential energy in the enclosure. ____
no control; _ _ potential energy; . . . . squared
pressure; _ . _ . energy density.

Figure 2. Attenuation of potential energy in the
enclosure. ____ potential energy; . . . . squared
pressure; _ _ energy density.

approaches can be obtained by looking at the pressure field that results when the control is applied. There are some frequencies where the global potential energy that results from control is comparable with all three methods. Due to space limitations, results for such cases are not shown here, but it has been found that the nature of the controlled field is rather similar for all three control methods. There are other frequencies characterized by a significant difference in the attenuation of the global energy achieved when minimizing the potential energy or energy density, as opposed to the squared pressure. One example of this is the spectral peak at 166.3 Hz, which corresponds to the (1,0,1) mode. It can be seen from Figure 2 that controlling the potential energy or energy density produces an attenuation of the potential energy in the range of 11-14 dB. However, controlling the squared pressure produces an increase of the potential energy of approximately 15 dB. Figures 3 and 4 show the relative sound pressure level for two different cross-sectional planes of the enclosure, given by $z = 0.8$ m and $z = 1.0$ m. For the (1,0,1) mode, the error sensor (located at $z = 0.6$ m) is near the nodal plane of the mode given by $z = 0.61$ m. As a result, if the squared pressure is controlled, the error sensor is largely incapable of detecting the dominant mode in the enclosure, and as a consequence, the control solution results in a general increase in the sound pressure levels throughout the enclosure. On the other hand, since the energy density control approach is also sensitive to velocity components of the modes, it is capable of detecting the dominant mode in the enclosure, and yields a much more satisfactory solution.

CONCLUSIONS

Three active control methods have been investigated to compare the global attenuation that can be achieved in a rectangular enclosure. For a given configuration, the method of controlling energy density often provides attenuation of the global energy in the field that is comparable to minimizing the overall potential energy. On the other hand, minimizing the squared pressure has a tendency to produce localized control effects, in which the pressure is attenuated significantly in the area of the error sensor, but at the expense of increasing the overall energy in the field.

ACKNOWLEDGEMENTS

REFERENCES
1.   S. J. Elliott, P. A. Nelson, I. M. Stothers, C. C. Boucher, J. Evers, and B. Chidley, *J. Sound Vib.*, **140**, 219-238 (1990).
2.   M. Paxton, M. Purver, C. F. Ross, M. Baptist, M. A. Lang, D. N. May, M. A. Simpson, *Second Conf. Recent Advances in Active Control of Sound and Vib.*, S100-S109 (1992).
3.   U. Emborg and C. F. Ross, *Second Conf. Recent Advances in Active Control of Sound and Vib.*, S67-S73 (1993).
4.   S. D. Sommerfeldt and P. J. Nashif, *Proc. Second Intl. Congress on Recent Developments in Air- & Structure-Borne Sound and Vib.*, 361-368 (1992).
5.   P. J. Nashif and S. D. Sommerfeldt, *Proc. Inter-Noise 92*, 357-362 (1992).
6.   P. A. Nelson, A. R. D. Curtis, S. J. Elliott and A. J. Bullmore, *J. Sound Vib.*, **117**, 1-13 (1987).
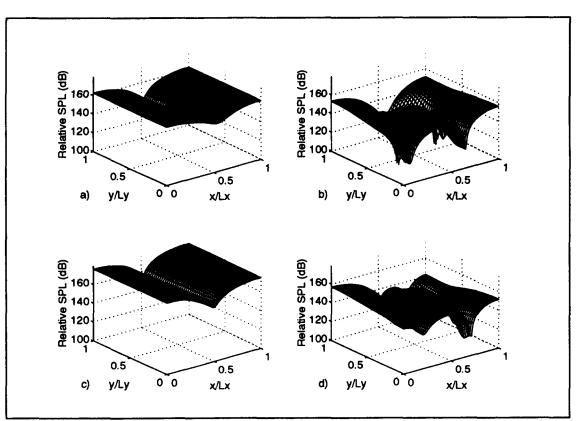
Figure 3. Relative sound pressure level in the z = 0.8 m plane: a) No control; b) Potential energy minimized; c) Squared pressure minimized; d) Energy density minimized.
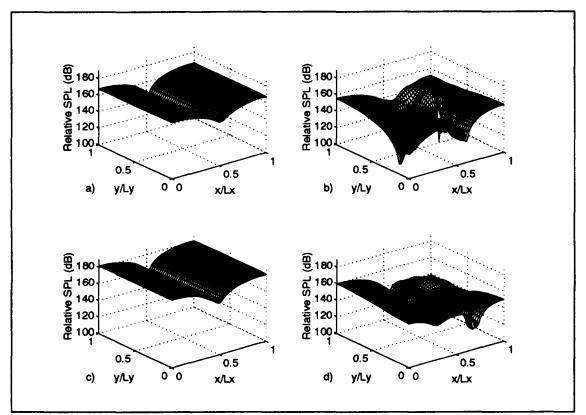

Figure 4. Relative sound pressure level in the z = 1.0 m plane: a) No control; b) Potential energy minimized; c) Squared pressure minimized; d) Energy density minimized.